

**Anelastic spectroscopy study of the metal-insulator transition of  $\text{Nd}_{1-x}\text{Eu}_x\text{NiO}_3$** F. Cordero,<sup>1</sup> F. Trequatrini,<sup>2</sup> V. B. Barbeta,<sup>3</sup> R. F. Jardim,<sup>4</sup> and M. S. Torikachvili<sup>5</sup><sup>1</sup>*CNR-ISC, Istituto dei Sistemi Complessi, Area della Ricerca di Roma - Tor Vergata, Via del Fosso del Cavaliere 100, I-00133 Roma, Italy*<sup>2</sup>*Dipartimento di Fisica, Università di Roma "La Sapienza", P. le A. Moro 2, I-00185 Roma, Italy*<sup>3</sup>*Departamento de Física, Centro Universitário da FEI, São Bernardo do Campo, 09850-901, Brazil*<sup>4</sup>*Instituto de Física, Universidade de São Paulo, CP 66318, São Paulo, 05315-970, Brazil*<sup>5</sup>*Department of Physics, San Diego State University, San Diego, California 92182-1233, USA*

(Received 6 June 2011; revised manuscript received 14 July 2011; published 15 September 2011)

Measurements are presented of the complex dynamic Young's modulus of  $\text{NdNiO}_3$  and  $\text{Nd}_{0.65}\text{Eu}_{0.35}\text{NiO}_3$  through the metal-insulator transition (MIT). Upon cooling, the modulus presents a narrow dip at the MIT followed by an abrupt stiffening of  $\sim 6\%$ . The anomaly is reproducible between cooling and heating in  $\text{Nd}_{0.65}\text{Eu}_{0.35}\text{NiO}_3$  but appears only as a slow stiffening during cooling in undoped  $\text{NdNiO}_3$ , in conformance with the fact that the MIT in  $R\text{NiO}_3$  changes from strongly first order to second order when the mean  $R$  size is decreased. The elastic anomaly seems not to be associated with the antiferromagnetic transition, which is distinct from the MIT in  $\text{Nd}_{0.65}\text{Eu}_{0.35}\text{NiO}_3$ . It is concluded that the steplike stiffening is due to the disappearance or freezing of dynamic Jahn-Teller (JT) distortions through the MIT, where the JT active  $\text{Ni}^{3+}$  is disproportionated into alternating  $\text{Ni}^{3+\delta}$  and  $\text{Ni}^{3-\delta}$ . The fluctuating octahedral JT distortion necessary to justify the observed jump in the elastic modulus is estimated as  $\sim 3\%$  but does not have a role in determining the MIT, since the otherwise-expected precursor softening is not observed.

DOI: [10.1103/PhysRevB.84.125127](https://doi.org/10.1103/PhysRevB.84.125127)

PACS number(s): 71.30.+h, 71.70.Ej, 62.40.+i, 75.50.Ee

**I. INTRODUCTION**

There is still uncertainty regarding the exact nature of the metal-insulator transition (MIT) in the  $R\text{NiO}_3$  perovskites.<sup>1-3</sup> Following a systematic study with several  $R$  ion sizes,<sup>4</sup> the MIT in these perovskites has been associated with the opening of a gap between the O  $2p$  band and the Ni  $3d$  upper Hubbard band when the  $R$  ion size and/or temperature are decreased.<sup>4,5</sup> In fact, the  $R$ -O bond is too short with respect to the Ni-O bond for the cubic perovskite structure, and the mismatch is relieved by tilting of the  $\text{NiO}_6$  octahedra. Both a smaller  $R$  size and cooling enhance the mismatch and hence tilting, for steric reasons and because of the larger thermal expansion of the  $R$ -O bond. This results in a further reduction of the angle between Ni-O-Ni bonds with respect to  $180^\circ$ , reduces the overlap and hence the width of the O  $2p$  and Ni  $3d$  bands, and finally opens a gap between them, causing the MIT.<sup>5</sup> Indeed, with increasing the  $R$  ion size the temperature  $T_{\text{IM}}$  at which the MIT occurs decreases or the metallic phase becomes more stable.<sup>4</sup> In this manner it is possible to rationalize the phase diagram of  $R\text{NiO}_3$  of  $T$  vs the  $R$  ion size, and a similar behavior is found in cobaltites.<sup>6</sup>

On the other hand,  $\text{Ni}^{3+}$  has an electronic configuration similar to that of  $\text{Mn}^{3+}$ , with filled  $t_{2g}$  triplet states (thanks to Hund's rule in the case of Mn) and one electron in the  $e_g$  doublet, whose degeneracy can be lifted by tetragonal and orthorhombic distortions according to the Jahn-Teller (JT) effect. The physics of Mn perovskites is dominated by the Jahn-Teller coupling between these  $e_g$  electronic states and the distortions of the octahedra, which is a cause of orbital ordering (OO), and the same might be expected for nickelates. On the contrary, according to the early diffraction experiments the octahedral distortions in nickelates are extremely small or null.<sup>5,7</sup> Later, starting with the nickelates with smaller  $R$ , it has been found that the MIT is accompanied by a subtle orthorhombic to monoclinic structural change, with charge

disproportionation (CD)  $2\text{Ni}^{3+} \rightarrow \text{Ni}^{3+\delta} + \text{Ni}^{3-\delta}$  and charge ordering (CO) into alternately expanded and contracted  $\text{NiO}_6$  octahedra along the three directions,<sup>8</sup> and some octahedral distortion of the larger  $\text{Ni}^{3-\delta}\text{O}_6$  octahedra. A similar result has been recently found also with the larger  $R$  ions Nd<sup>9</sup> and Dy.<sup>10</sup> Such JT distortions are found only in the larger and more ionic  $\text{Ni}^{3-\delta}\text{O}_6$  octahedra and are at least 1 order of magnitude smaller than those observed in manganites.

Notice that in a naive picture CO and OO should not occur in the same set of Ni ions, since  $\text{Ni}^{3+}$  is JT active while  $\text{Ni}^{2+}$  and  $\text{Ni}^{4+}$  are not, but to what extent CO and OO occur in nickelates is still subject of controversy. Just because of the subtleness of the structural changes attributable to CO or OO, recourse has been had to resonant X-ray scattering.<sup>11-14</sup> These experiments in  $\text{NdNiO}_3$  are interpreted as evidence of partial CO rather than OO occurring at the MIT. According to this view, the degeneracy of the  $e_g$  orbitals would be lifted already in the metallic state, where the OO would be reflected by the tilts of the octahedra; the MIT would be due only to CD, accompanied by a small change of tilt angle.<sup>13</sup> It is debated to what extent these experiments may provide information on the contribution of CO and OO to MIT,<sup>15</sup> but the view that MIT is due to CO rather than OO received further support from theory and experiments under hydrostatic pressure in  $\text{LuNiO}_3$ ,<sup>16</sup> and from the above mentioned diffraction studies on  $R = \text{Nd}$  and  $\text{Eu}$ , where alternated small and large octahedra are found.<sup>9,10</sup> Nonetheless, recent experiments under pressure<sup>17</sup> suggest that the previous ones<sup>16</sup> were affected by an unwanted uniaxial component of pressure, and exclude a role of CO in the MIT,<sup>17</sup> rather, dynamic JT deformations would be responsible for large isotope effects in  $T_{\text{IM}}$ .<sup>18</sup>

Additional experiments that have been performed in order to probe CD with CO and OO at the MIT in nickelates include Mössbauer<sup>19-22</sup> and x-ray absorption spectroscopies.<sup>23</sup> Again, there is no clear picture, with possibility of OO<sup>19,20</sup> or CO<sup>20-22</sup> even in the metallic state.<sup>23</sup>

A similarly confused situation exists for  $\text{NaNiO}_2$  and  $\text{LiNiO}_2$ , which are also composed of  $\text{NiO}_6$  octahedra but sharing the edges instead of corners.<sup>24</sup> While  $\text{NaNiO}_2$  undergoes a phase transformation with clear cooperative JT distortion,  $\text{LiNiO}_2$  has little or even reverse JT distortion,<sup>25</sup> which is not yet explained. Some of the proposed explanations involve the peculiar geometry of the  $\text{LiNiO}_2$  lattice, where the triangular Ni sublattice frustrates AFM correlations, but other possible causes may apply also to  $\text{RNiO}_3$ , like the fact that the JT distortion exists but is incoherent<sup>26</sup> or with very short coherence length,<sup>25</sup> or is hindered by the electron delocalisation.<sup>16</sup>

From the above summary and recent reviews<sup>1</sup> it appears that, in spite of the wealth of experimental data on the  $\text{RNiO}_3$  series, the presence and role of CD and CO and/or OO at the MIT is not clear. In the Mn perovskites important and quantitative information has been obtained on such issues by studying the associated elastic anomalies;<sup>27,28</sup> in Ni perovskites no such type of investigation has ever been reported, except for a preliminary report of the present results.<sup>29</sup> Here anelastic spectroscopy measurements on  $\text{Nd}_{1-x}\text{Eu}_x\text{NiO}_3$  are presented and discussed, which shed new light on these issues.

## II. EXPERIMENTAL

Polycrystalline samples of  $\text{Nd}_{1-x}\text{Eu}_x\text{NiO}_3$  ( $x = 0$  and 0.35) were prepared from sol-gel precursors, sintered at  $T = 1000$  °C, and under oxygen pressure of 80 bar. Details of the synthesis process for preparing these samples are described in details elsewhere.<sup>30</sup> All samples were characterized by X-ray powder diffraction in a Bruker D8 Advance diffractometer. The x-ray diffraction patterns showed no extra reflections due to impurity phases, and indicated that all samples have a high degree of crystallinity. The samples were two bars with  $x = 0$  (NEN0) and with  $x = 0.35$  (NEN35), both with approximate size  $43 \times 6 \times 0.7$  mm<sup>3</sup> and a density  $\rho \simeq 2.9(3.1)$  g/cm<sup>3</sup> for NEN0(35), about 40% of the theoretical density. Such a high porosity makes the evaluation of the absolute value of the complex Young's modulus  $E = E' + iE''$  problematic, but did not affect the quality of the measurement of its temperature dependence. This was measured by electrostatically exciting the flexural vibrations of the bars, which were suspended on thin thermocouple wires in vacuum, and with one face made well conducting also below the MIT with Ag paint. It was possible to excite various flexural modes, whose resonance frequencies are ideally in the ratios  $f_{1F} : f_{2F} : f_{3F} : f_{5F} = 1 : 2.800 : 5.487 : 13.55$ . The fundamental frequency is given by<sup>31</sup>

$$f_{1F} = 1.028 \frac{h}{l^2} \sqrt{\frac{E}{\rho}} \quad (1)$$

where  $l$  is the length,  $h$  the thickness,  $\rho$  the density of the bar; at room temperature it was  $f_{1F} \sim 0.6 - 1$  kHz.

In the Discussion we will need an estimate of the absolute value of the Young's modulus, which is found with Eq. (1). The effective Young's moduli at room temperature, uncorrected for porosity, were  $E = 4.5$  GPa for NEN0 and 12.5 GPa for NEN35, which are 5–10 times smaller than the typical values  $E \sim 100$  GPa found in ceramics of similar type. Sources of error are the sample porosity, deviations from the shape

of a rectangular parallelepiped, low homogeneity and the presence of the Ag conductive layer, wrong identification of the vibration modes and mixing of flexural with torsional modes. The largest source of error in our case seems to be the extremely high porosity,  $p \simeq 0.60$ . The other causes should be of minor importance; for example, the NEN0 sample had the lowest value of  $E$ , but its ratios  $f_{3F}/f_{1F} = 5.60$  and  $f_{5F}/f_{1F} = 13.66$  were in excellent agreement with the theoretical values given above. The correction for such high porosities are very unreliable; to give an idea, the Young's modulus of porous ceramics are corrected with empirical expressions like  $(1 - p)^n$  with  $n \simeq 1$ ,<sup>32</sup> or  $\exp(-bp)$  with  $2.1 < b < 2.8$ .<sup>33</sup> These expressions would enhance  $E$  in our case by a factor between 2.5 and 5.2. While this brings  $E$  of NEN35 to reasonable values up to 66 GPa, the value of NEN0 would remain below 25 GPa. The large difference between the two may in part be accounted for by different types of porosities, in terms of shape and connectivity of the pores, and in part due to the Eu substitution. In the discussion we will assume  $E \sim 65$  GPa.

The anelastic spectra are displayed in terms of the real part of the Young's modulus or its reciprocal, the compliance  $s = E^{-1} = s' - is''$ , and of the elastic energy loss coefficient  $Q^{-1} = s''/s'$ .

## III. RESULTS

In Fig. 1 is reported the anelastic spectrum of NEN0 measured during cooling (empty symbols) and subsequent heating (filled symbols) measured exciting the first odd flexural modes at 0.63, 3.5 and 8.6 kHz during the same run. During cooling, below 190 K there is a progressive stiffening of the Young's modulus in excess of the slight linear anharmonic stiffening observed at higher temperature; such a stiffening proceeds until the lowest temperature reached by us, although in the end it starts levelling off. On heating, the modulus resumes the almost linear and weak temperature dependence except for a steplike softening followed by a dip at 191 K. It is clear by comparison with resistivity, specific heat and magnetization measurements that the steplike change of  $E(T)$  with large temperature hysteresis is due to the MIT.<sup>29,34</sup>

The  $Q^{-1}(T)$  is perfectly reproducible on heating and cooling, except for the sharp peak in correspondence with the cusped softening, both of which appear only during heating. In addition, there are other three peaks: P1 at 230–240 K, P2 at 171 K and P3 at 100–110 K. While the temperature of P2 is independent of frequency, the other two increase with frequency, and therefore indicate thermally activated processes whose maxima occur when the condition  $\omega\tau \simeq 1$  is met,<sup>31</sup> where  $\omega/2\pi$  is frequency and  $\tau(T)$  a relaxation time. We will ignore these reproducible but small peaks.

The spectrum of NEN35 (Fig. 2) is similar to that of NEN0 during heating, but the MIT occurs at  $T_{\text{IM}} = 288$  K, if identified with the cusp in the real part, and the hysteresis is completely absent, the only difference between heating and cooling being the intensity of the peak in real and imaginary parts at the MIT. The curves measured at a frequency five times higher are not shown for clarity, since they are identical except that the peak in  $Q^{-1}$  is  $\sim 15\%$  higher, whereas in NEN0 it is nearly identical.

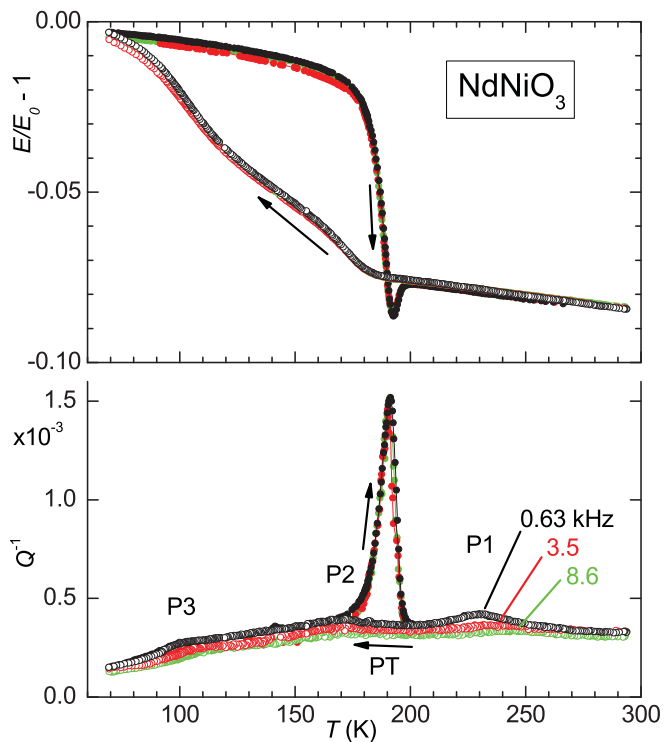


FIG. 1. (Color online) Young's modulus  $E$  and elastic energy loss coefficient  $Q^{-1}$  of NEN0 measured on cooling (empty symbols) and heating (filled symbols) at 0.63 kHz (black), 3.5 kHz (red) and 8.6 kHz (green).

The other small peaks in the  $Q^{-1}$  are absent in NEN35. In Fig. 2 are also reported the curves measured on NdNiO<sub>3</sub> during heating, rescaled in temperature by a factor 1.504. The rescaled elastic anomaly of NdNiO<sub>3</sub> is slightly sharper and narrower in the real part, with a smaller dip, and almost coincident in the absorption. In NEN35 the antiferromagnetic (AFM) transition occurs at  $T_N = 240$  K  $<$   $T_{IM}$ ,<sup>29</sup> but there is no clear sign of it in the anelastic spectra.

#### IV. DISCUSSION

The overall phenomenology of the anelastic anomalies found in Nd<sub>1-x</sub>Eu<sub>x</sub>NiO<sub>3</sub> appears to be mainly related to the MIT and in agreement with what is known from other techniques. In NdNiO<sub>3</sub> the MIT occurs at  $T_{IM} = T_N \simeq 192$  K and has marked first order character, with a large hysteresis between cooling and heating. When decreasing the mean  $R$  ion size by Eu doping, the MIT shifts to higher temperature and becomes second order, while  $T_N$  shifts below  $T_{IM}$ . The anelastic anomalies also appear to be marginally affected by the magnetic transition, since the heating curves are very similar to each other regardless of the fact that  $T_N$  coincides with  $T_{IM}$  or not. The present data can be compared with those of resistivity, magnetization and specific heat taken on the same materials.<sup>29,34</sup> The hysteresis is due to the fraction of material that remains metallic in the insulating phase, and the fact that the step in  $\rho(T)$  (see Fig. 7 in Ref. 34) is narrower than that in  $E(T)$  during cooling is explained by the fact that the latter probes the bulk fraction of insulating and metallic

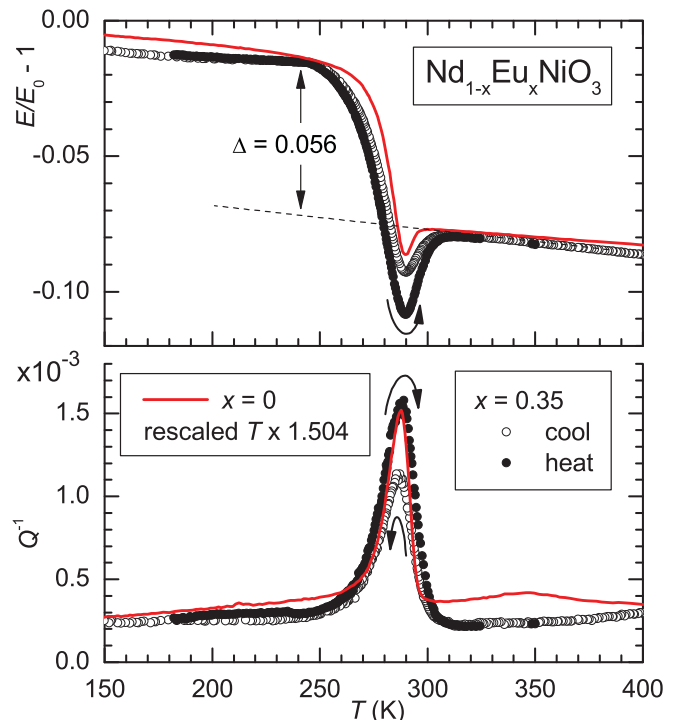


FIG. 2. (Color online) Young's modulus  $E$  and elastic energy loss coefficient  $Q^{-1}$  of NEN35 measured on cooling (empty symbols) and heating (filled symbols). For comparison, the anelastic spectrum of NEN0 on heating is reported (line) after scaling its temperature to let its  $T_{IM}$  coincide with that of NEN35.

phases, while resistivity rather probes percolating conductive paths.

#### A. Comparison with the specific heat anomaly

It seems that the dip in the modulus at  $T_{IM}$  and the stiffening below it have different origins, since with  $x = 0.35$  the dip and accompanying peak in  $Q^{-1}$  differ in amplitude between heating and cooling, while the step in  $E$  is reproducible. This observation allows us to separate the two anomalies and compare the dip in the modulus, or peak in compliance  $s = E^{-1}$ , with the peak in specific heat. The curves 1 and 2 in Fig. 3 are the normalized compliance on heating and cooling, after subtracting a linear background  $s_{bg}$ ; the reference  $s_0$  is the extrapolation of  $s_{bg}$  to 0 K. Besides the peak at 290 K and the step below that temperature, there is an additional shallow rise of the compliance below 250 K. The shape of the latter is very uncertain, due to the background subtraction. The anharmonic phonon contribution to the temperature dependence of the elastic constants is generally almost linear and levels off at low temperature, but being unable to distinguish the anharmonic contribution from the other anomalies in the temperature dependence of  $s$ , we chose to use a simple linear interpolation over the whole 60–350 K range. Curve 3 is the difference between curves 1 and 2 and it has been subtracted from them after multiplication by scale factors in order to remove the peaked component. It turns out that the best values of the factors are 2.00 and 1.00. The resulting curves 4 and 5 are coincident and have only the step below 290 K plus the shallow rise.

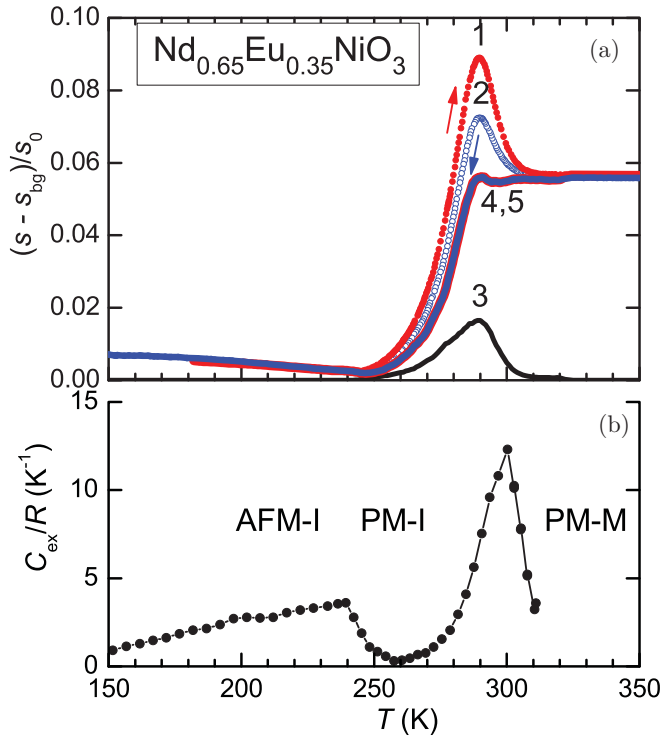


FIG. 3. (Color online) (a) Curves 1 and 2: compliance  $s = E^{-1}$  of NEN35 after subtraction of the anharmonic background  $s_{bg}$ , measured on heating and cooling. Curve 3 is the difference between them,  $s_{peak}$ . Curve 4 and 5 are curves 1 and 2 after subtraction of the peaked component 3. (b) Excess specific heat extracted from Ref. 29.

Both the peak  $s_{peak}$  (curve 3) and the excess compliance below 250 K can be put in relationship with the excess specific heat  $C_{ex}$  measured on a similar sample.<sup>29</sup> In fact, a softening proportional to the specific heat anomaly is expected at a magnetic transition,<sup>35</sup> and also at other types of transitions under the rather general condition that their critical temperature depends on pressure or more generally on stress.<sup>36</sup> A possible identification of the two anomalies in  $C_{ex}$  is the peak at  $\sim 300$  K with the CO and/or orbital transition concomitant with the MIT, possibly with participation of spin degrees of freedom,<sup>37</sup> and the broad contribution below 250 K with the onset of long range AFM order. The latter is expected to produce a jump  $\Delta S = R \ln 2$  in the entropy of the  $S = \frac{1}{2}$  spins,<sup>38,39</sup> but the jumps of the entropy  $S = \int dT C_{ex} / T$  are only  $\Delta S = 0.15R$  between 130 and 260 K and  $\Delta S \simeq 0.12R$  between 260 and 320 K. The fact that the actual step is smaller than expected from complete AFM ordering has already been noted in other  $RNiO_3$  nickelates, and has been interpreted as due to AFM correlations also above  $T_N$ , so that only a relatively small loss of entropy is involved in the long range AFM ordering.<sup>38,39</sup>

### B. Step-like stiffening below the MIT

The main feature of the elastic anomaly at both compositions is the stiffening below the MIT, whose step-like nature is made evident after the subtraction of the peaked component in curves 4 and 5 of Fig. 3. This is quite an unusual observation, since phase transitions are generally accompanied

by softening rather than stiffening. As discussed below, if some strain component is coupled linearly with the order parameter of the transition, then its elastic constant presents a cusped softening at the critical temperature and is therefore followed by restiffening to the background elastic constant on further cooling. This is not the case of curves 4 and 5, which lack any sign of precursor softening divergent near  $T_{IM}$ .

There are several elastic studies of the CO and OO transitions in perovskite manganites and in other compounds, but most of them concentrate on the precursor softening above the transitions. In few cases the subsequent restiffening below the transitions has been considered, especially if it appears of excessive sharpness and amplitude with respect to the precursor softening. In these cases recourse has been had to different sets of fitting parameters above and below  $T_{CO}$ ,<sup>40</sup> or to a Landau free energy expansion with coefficients unrelated to CO or OO.<sup>41</sup> In  $Nd_{0.5}Sr_{0.5}MnO_3$  a steplike stiffening at the MIT has been interpreted as the effect of the renormalisation of the elastic constant by the conduction electrons with a factor  $(1 + g^2 \chi(T))^{-1/2}$ , where  $g$  is the electron-phonon coupling constant and  $\chi(T)$  is the electron susceptibility, identified with the magnetic susceptibility  $\chi_m$ .<sup>42</sup> In that case, the MIT coincides with a transition from FM to AFM and  $\chi_m$  has a negative step, which becomes positive in the renormalisation factor of the elastic constant. This type of analysis is not appropriate to  $Nd_{1-x}Eu_xNiO_3$ , whose magnetic susceptibility has an almost imperceptible decrease below  $T_N$ , superimposed to a stronger rise with cooling, even after subtraction of the contribution of the Nd and Eu ions.<sup>34,43</sup>

Lacking an adequate precedent for a satisfactory interpretation of the step component of the elastic compliance of  $Nd_{1-x}Eu_xNiO_3$ , we first review what kind of elastic response is expected at a MIT or magnetic transition, and then propose an interpretation based on the response of the JT distortions, from a point of view different from that usually adopted. Detailed discussions of the elastic anomalies expected at various types of phase transitions can be found in many review articles and books, usually based on the Landau theory with the coupling between strain and order parameter included,<sup>44-48</sup> and therefore we only quote what is strictly necessary to our discussion.

### C. Landau analysis

Near a phase transition the free energy can be expanded in powers of the order parameter(s)  $Q$ . In the present case the order parameter (OP) can be one or more of the symmetrized charge fluctuation coordinates for describing charge ordering, or the quadrupolar orbital operators of the Ni ions for orbital ordering, or the staggered magnetization for the AFM transition. By including powers of  $Q$  up to the 6th order, it is possible to reproduce both first and second order transitions, and including coupling terms containing both  $Q$  and strain  $\varepsilon$ , it is possible to deduce the effect of the relaxation of the OP under stress on the elastic constants. In the case that the OP is strain itself or is linearly coupled to it with a term  $\lambda \varepsilon Q$ , the elastic constant coupled to the OP ideally vanishes at the transition temperature  $T_C$ , or at least has a negative cusp. If bilinear coupling is forbidden because no strain has the same symmetry of the OP, the next coupling term,  $\mu \varepsilon Q^2$ , causes a



negative step at  $T_C$  in the the elastic constant coupled to the OP, possibly including a weak restiffening below  $T_C$ . A biquadratic coupling  $\nu\epsilon^2 Q^2$  adds to the elastic constant a contribution  $2\nu\langle Q^2 \rangle$  below  $T_C$ , which can be a linear or saturating rise or decrease, depending on the temperature dependence of the OP and on the sign of the coupling constant  $\nu$ . Of all these terms, the latter is the only one that might produce a stiffening below  $T_C$  without precursor softening; other terms are possible but less important in the great majority of cases.

#### D. Magnetic transition

Magnetic transitions cause elastic anomalies through essentially two mechanisms: exchange striction and magnetostriction. The first mechanism causes cusp-like softening in the elastic constants involving the strains that change the atomic distances and hence the exchange constant. The magnitude of such anomalies is of the order of 1%.<sup>48</sup> Even smaller step-like softening can be caused by magnetostrictive coupling with the lattice, namely by a term  $-B\epsilon_{ij}S_iS_j$  linear in strain and quadratic in spin variable or magnetization, which, according to Landau's theory,<sup>44</sup> produces below the magnetic transition a negative step in the modulus  $M$  of magnitude  $-2B^2/M$ . Such a softening is usually observed at magnetic transitions.<sup>35,49,50</sup>

On the other hand, in the FM transition of  $\text{YTiO}_3$ , a stiffening is found,<sup>51</sup> whose origin has not been explained, but also involves OO. In the hexagonal quasi-1D AFM multiferroic  $\text{YMnO}_3$ , there is 1% stiffening below  $T_N$  in  $C_{11}$  and 3% in  $C_{66}$  due to biquadratic coupling<sup>52</sup> (see previous paragraph). In fact, below  $T_N = 75$  K the temperature dependence of  $\Delta C_{ii}(T)/C_{ii}$  follows the squared OP,  $S^2 \propto (1 - T/T_N)^{2\beta}$ , down to 2 K, which appears different from the abrupt rise in  $\text{Nd}_{1-x}\text{Eu}_x\text{NiO}_3$ . In the present case, the involvement of magnetic effects in the steplike stiffening is made even more unlikely by the fact that in  $\text{Nd}_{0.65}\text{Eu}_{0.35}\text{NiO}_3$  the magnetic transition occurs at  $T_N < T_{\text{IM}}$ .

#### E. Cooperative Jahn-Teller phase transition and orbital ordering

Following the notation of Hazama and coworkers,<sup>27,28</sup> the quadrupolar moments of the  $e_g$  orbitals of  $\text{Ni}^{3+}$  can couple with tetragonal  $\epsilon^u = (2\epsilon_{zz} - \epsilon_{xx} - \epsilon_{yy})/\sqrt{3}$  and orthorhombic  $\epsilon^v = \epsilon_{xx} - \epsilon_{yy}$  strains (both with the same  $E_g$  elastic constant  $C' = (C_{11} - C_{12})/2$ ), and interact with each other causing the cooperative JT transition.<sup>53</sup> The relevant part of the Hamiltonian of  $N$   $\text{Ni}^{3+}$  ions per unit volume, referred to the unit cell volume  $v_0$ , is

$$H = -v_0N \sum_{\gamma=u,v} g_\gamma O_\gamma \epsilon^\gamma - v_0N \sum_{\gamma=u,v} g' \langle O_\gamma \rangle O_\gamma \quad (2)$$

where the quadrupolar operators  $O_2^0 = (2l_z^2 - l_x^2 - l_y^2)/\sqrt{3}$  and  $O_2^2 = l_x^2 - l_y^2$  correspond, apart from a geometrical factor  $a = \langle \phi_{eg} | O_{eg} | \phi_{eg} \rangle = 2\sqrt{3}$ , to the occupation numbers of octahedra with tetragonal and orthorhombic JT distortions reflecting the symmetry of their  $3d$  orbitals. The first term is the linear coupling to the external strain, with a coupling strength  $g$ , and causes softening of the  $C'$  elastic constant, while the second term is the elastic interaction among the orbitals in the mean field approximation with strength  $g'$ , and

determines the type of OO. The resulting softening of the  $C'$  elastic constant is

$$C' = C'_0 - Ng^2 \frac{\chi(T)}{1 - g'\chi(T)} \quad (3)$$

where  $C'_0$  is the background elastic constant and the susceptibility

$$\chi(T) = \frac{a^2}{k_B T} \quad (4)$$

is proportional to the contribution to the compliance  $s = C^{-1}$  from noninteracting orbitals,  $\Delta s(T) = (\frac{g}{C'})^2 \chi(T)$ . Equation (3) can be rewritten as

$$C' = C'_0 \left( \frac{T - T_{\text{OO}}}{T - \Theta} \right), \quad (5)$$

where  $\Theta = a^2 g'/k_B$ ,  $T_{\text{OO}} = \Theta + T_{\text{JT}}$  and  $T_{\text{JT}} = Na^2 g^2 / (k_B C'_0)$ . In this form it is clear that the elastic constant vanishes at  $T_{\text{OO}}$ , which is the onset of the OO or cooperative JT transition, and that stiffens again on further cooling. At higher temperatures, when  $T \gg \Theta$  and hence  $g'\chi(T) \ll 1$ , Eq. (3) shows that the softening induced by the orbitals freely responding to the applied stress is simply given by Eq. (4) and is  $\propto 1/T$ .

#### F. Charge ordering

The charge fluctuations can be expanded into fluctuation modes  $Q_\gamma$  acting as OP of the CO transition, one or some of which may be linearly coupled to the strain  $\epsilon_\gamma$  having the same symmetry with terms  $-g_\gamma Q_\gamma \epsilon_\gamma$ . As also shown in Appendix B, if such terms are included in the expansion of the free energy in powers of  $Q_\gamma$  up to the fourth order, a second order transition at a temperature  $T_{\text{CO}}$  results, and the renormalized elastic constant can be written exactly as in the case of the OO transition, Eq. ((5)), where  $\Theta$  is the temperature at which the term  $\frac{\alpha_0}{2}(T - \Theta)Q_\gamma^2$  of the Landau expansion vanishes and  $T_{\text{CO}} = \Theta + \Delta T$ ,  $\Delta T = g^2/(\alpha_0 C_\gamma)$ , with  $C_\gamma$  the elastic constant appropriate to  $\epsilon_\gamma$ , is the temperature at which the CO transition occurs with onset of spontaneous strain of type  $\epsilon_\gamma$ . Therefore, OO between two orbitals and CO from condensation of a single charge fluctuation mode produce the same precursor softening on the appropriate elastic constant  $C_\gamma$  ( $= C'$  for OO within the  $e_g$  doublet). The restiffening below the transition is discussed in Appendix B. Examples of materials similar to  $\text{RNiO}_3$  where both transitions have been recognized in ultrasonic experiments are  $\text{La}_{1-x}\text{Sr}_x\text{MnO}_3$  with  $T_{\text{CO}} < T_{\text{OO}}$ <sup>27</sup> and  $\text{Pr}_{1-x}\text{Ca}_x\text{MnO}_3$  with  $T_{\text{CO}} > T_{\text{OO}}$ .<sup>28</sup>

#### G. Softening in terms of octahedral JT distortion and its disappearance below the MIT

From the above discussion it appears that a transition whose driving force is the interaction between JT active orbitals or between ionic charges would appear in the coupled elastic constant as a clear precursor softening that diverges at the transition, followed by restiffening on further cooling. This is clearly not the case of  $\text{Nd}_{1-x}\text{Eu}_x\text{NiO}_3$ , since the Young's modulus presents a weak and almost linear stiffening down to a temperature very close to the MIT, which excludes any

mechanism coupled to strain. This is also shown quantitatively in Sec. I.

The picture we propose is the following. The MIT is an electronic transition, presumably occurring at the opening of the charge transfer gap during cooling,<sup>4,5</sup> when the  $R-O$  bonds, having larger thermal expansion of the shortest Ni-O bonds, shorten faster than the latter and enhance the buckling of the Ni-O-Ni bonds beyond a critical threshold. The driving mechanism for this is the thermal contraction due to lattice anharmonicity, and there is no effect on the elastic constants other than the usual anharmonic stiffening. In the metallic phase the octahedra would be JT distorted with a fluctuation rate much faster than our measuring frequency, so that their contribution to the lattice softening would be noncritical, namely Eq. (3) with  $g' = 0$ , and the OO transition would occur well below  $T_{IM}$ . *The MIT would inhibit such a softening, possibly due to the concomitant CO that transforms JT active  $Ni^{3+}$  into (partially) inactive  $Ni^{3\pm\delta}$ , or making the distortions static, or both. This would make the insulating phase stiffer than the metallic one,* so that the disappearance of the metallic phase would be accompanied by elastic stiffening.

In what follows we will evaluate the JT distortion necessary to explain the steplike stiffening in Figs. 1 and 2 with the above mechanism and test the consistency of this explanation with the available data. In order to relate the amount of elastic softening to the JT distortion of the octahedra, rather than to the coupling coefficient  $g$ , it is convenient to recast the above results in the usual formalism of anelastic relaxation from point defects.<sup>31,54</sup> It may seem unrealistic to describe distorted octahedra sharing the O atoms, and hence strongly interacting, as almost independent defects carrying a distortion, but this is equivalent to the formulation of Sec. IV E, namely the OO approach to the cooperative JT effect.<sup>55</sup> In the case of nickelates it is certainly justified by the smallness of the JT distortions, which make uncorrelated fluctuations less energetically unfavorable. If we neglect the interaction term  $\propto g'$ , the hamiltonian ((2)) is equivalent to that of a system of independent defects of type  $\gamma = u, v$  with double-force tensor  $p^\gamma$ , whose interaction energy with an external strain  $\varepsilon$  is<sup>56</sup>

$$E = -v_0 \sum_{\gamma} \sum_{ij} c_{\gamma} p_{ij}^{\gamma} \varepsilon_{ji}$$

where  $c_{\gamma}$  with  $\sum_{\gamma} c_{\gamma} = v_0 N$  are the molar concentrations of defects, and the summation over the cartesian components  $i, j$  selects the strain component of the same symmetry of the defect,  $\varepsilon^{\gamma}$ . It appears therefore that  $N g_{\gamma} O_{\gamma}$  in Eq. (2) is equivalent to  $c_{\gamma} p^{\gamma}$ , although the separate correspondences  $N O_{\gamma} \rightarrow c_{\gamma}$  and  $g_{\gamma} \rightarrow p^{\gamma}$  do not necessarily hold. In turn, the double force tensor can be expressed in terms of the elastic quadrupole  $\lambda_{ij}^{\gamma}$  (usually called elastic dipole<sup>31</sup>) as  $p_{ij}^{\gamma} = \sum_{kl} C_{ijkl} \lambda_{kl}^{\gamma}$ , where  $C$  is the fourth-rank elastic stiffness tensor. The tensor  $\lambda^{\gamma}$  is adimensional and is the strain of a unity concentration of defects of type  $\gamma$ , in the present case the tetragonal or orthorhombic strain of the octahedra, so that the anelastic strain due to defects is

$$\varepsilon^{an} = \sum_{\gamma} c_{\gamma} \lambda^{\gamma},$$

where the  $c_{\gamma}$  obey Boltzmann's statistics and depend on the applied stress  $\sigma$  through the defect energies  $E_{\gamma} = -v_0 p^{\gamma} \varepsilon_{\gamma} = -v_0 \lambda^{\gamma} \sigma_{\gamma}$ . For only two types of defects with the same symmetry and coupled to strain through the same symmetrized elastic constant  $C'$  the relationship between  $\lambda$  and  $p$  is simply  $\lambda = p/C'$ , and the contribution to the compliance,  $s' = 1/C'$ , is<sup>31,54</sup>

$$\delta s' = \frac{d\varepsilon^{an}}{d\sigma} \propto c \frac{(\Delta\lambda)^2}{k_B T} \quad (6)$$

where  $\Delta\lambda = |\lambda_u - \lambda_v|$  and the numerical factor differs from those usually reported for reorientation of defects with the same symmetry, since we are dealing with the relaxation between a tetragonal and an orthorhombic state rather the reorientation of the principal axes of  $\lambda$  among equivalent crystallographic directions.

We can carry the analogy with point defects further into the dynamic response. If  $\tau$  is the relaxation time for an electron to change orbital, the softening Eq. (6) acquires a frequency dependent factor  $(1 + i\omega\tau)^{-1}$  noticeable when temperature is lowered enough to slow  $\tau^{-1}$  and make it comparable to the measuring angular frequency  $\omega$ ;<sup>31</sup> this has also been discussed in connection with JT effect in  $UO_2$ .<sup>57</sup> The concentration  $c$  of  $e_g$  electrons would be 1 for  $RNiO_3$  if there were no disproportionation of  $Ni^{3+}$ . The MIT may reduce the magnitude of  $\delta s'$  both reducing  $c$  through the concomitant disproportionation of  $Ni^{3+}$  and/or making null the frequency factor if the distortions become quasistatic with  $\omega\tau \gg 1$ .

In Appendix A we define the octahedral distortions in terms of the symmetrized tetragonal and orthorhombic strains  $T^u$  and  $T^v$  with magnitude  $\lambda$ , and evaluate the resulting polycrystalline average of the relaxation strength of the Young's modulus,  $\Delta = \delta E^{-1}/E^{-1}$ , as

$$\langle \Delta \rangle \simeq \frac{c v_0 \lambda^2}{15 k_B T} E. \quad (7)$$

#### H. Estimate of the Jahn-Teller distortion necessary to explain the stiffening below the MIT

As a first check that this mechanism can explain the stiffening at the MIT, let us suppose that on passing across the MIT the JT distortion totally disappears together with the  $Ni^{3+}$  ions; therefore we equate the above  $\langle \Delta \rangle$  with  $c = 1$  to the overall jump of  $\delta s/s_0 \simeq \delta E/E_0$ . The largest source of error in evaluating  $\lambda$  is the absolute value of the Young's modulus, which we assume to be  $E \sim 65$  GPa (see Sec. II), and together with  $\Delta = 0.056$  for NEN35 yields  $\delta E^{-1} \simeq 10^{-13} \text{ cm}^3/\text{erg}$ ; the cell volume is<sup>34</sup>  $v_0 = 55 \times 10^{-24} \text{ cm}^3$  and Eq. (7) with  $T = T_{IM}$  gives  $\lambda \simeq 0.031$ , namely 3% octahedral and tetragonal distortions.

In order for this interpretation to be selfconsistent, it should turn out that the temperature  $T_{OO} = \Theta + T_{JT}$  for OO is smaller than  $T_{IM}$ . There is no constraint to the smallness of the intersite contribution  $\Theta$ , which can also be negative for antiferroquadrupolar coupling. Instead, the JT energy is determined by the coupling with uniform strain,  $\lambda$ , with  $T_{JT} = N a^2 g^2 / k_B C'_0$ , where  $g$  is determined by the equivalence  $N g a \equiv c p = c C' \lambda$ . The  $C'_0$  elastic constant is unknown and we set it equal to  $E$ , finding  $g/k_B \simeq 2300$  K and  $T_{JT} = 240$  K,

therefore smaller than  $T_{IM}$ . The same estimate for  $NdNiO_3$  with  $\Delta = 0.062$  and  $T = 190$  K yields  $\lambda = 0.026$ ,  $g/k_B \simeq 1900$  K and  $T_{JT} = 177$  K, again smaller than  $T_{IM}$ .

Up to now it is shown that a CD with complete suppression of the JT effect can explain the stiffening below the MIT, but it is also necessary to determine the effect of an incomplete charge disproportionation  $2Ni^{3+} \rightarrow Ni^{3+\delta} + Ni^{3-\delta}$  with  $\delta < 1$ . The above treatment suggests a naive analogy of JT active octahedra with point defects, whose concentration is  $c = 1$  in the conductive phase and becomes  $c = 1 - \delta$  in the insulating one, with unchanged distortion  $\lambda$ . However, this is not the picture proposed after the diffraction experiments, where  $\delta$  is deduced from the change of valence of  $Ni^{3+}$ , and this is in turn extracted from the average Ni–O bond lengths together with the bond valence model.<sup>9</sup> In this picture, all the octahedra undergo disproportionation, and are alternated along the three principal directions as small  $Ni^{3+\delta}$  and large  $Ni^{3-\delta}$  octahedra, only the latter supporting some residual JT distortion.<sup>9,10</sup> From this point of view, a more sensible hypothesis is that, when entering the insulating phase, in Eq. (7)  $c$  passes from 1 to 1/2 and the JT distortion  $\lambda$  is reduced by an amount depending on  $\delta$ . If we suppose a linear relationship between  $\lambda$  and  $\delta$ , then we should set  $\lambda \rightarrow \lambda(1 - \delta)$  into Eq. (7), and repeating the above analysis with the estimate  $\delta \simeq 0.28$  for  $NdNiO_3$ ,<sup>9,11</sup> and  $c = 1/2$  we would find  $\lambda = 0.036$  and  $T_{JT} = 330$  K. The latter value, being slightly larger than  $T_{IM}$ , seems at first inconsistent with the present analysis, but there are several arguments that this is not necessarily the case. A first point is that we ignored the correlations between octahedra, which in the perovskite structure with octahedra sharing the vertices is expected to be antiferroelastic<sup>58</sup> and corresponds to a negative  $\Theta$  compensating  $T_{JT}$ , as in  $Pr_{1-x}Ca_xMnO_3$ .<sup>28</sup> Another point is that the JT distortion may not fall linearly with  $\delta$  but faster. Finally, if the JT distortions remained frozen below the MIT, then the kinetic factor  $1/[1 + (\omega\tau)^2]$  would pass from 1 to 0 on crossing the MIT and the initial safe estimate of  $\lambda$  of Eq.(7) with  $c = 1$  would again be correct.

Once established that the stiffening below the MIT can be consistently explained by vanishing or blocking of dynamic JT distortions  $\lambda$ , it is necessary to check the compatibility of such disordered distortions above  $T_{IM}$  with the structural studies on  $NdNiO_3$ . We refer to the most recent experiment with synchrotron powder-diffraction,<sup>9</sup> where the Ni–O bond lengths are reported to be  $l \simeq 1.9$  Å, and the B-factors of the apical and equatorial O atoms are 0.72 and 1.13 Å<sup>2</sup> at room temperature, resulting in thermal plus disordered displacements of 0.1 and 0.12 Å respectively. The JT distortions estimated here of  $\lambda \sim 0.03$  require changes of the bond lengths of  $\delta l = \lambda \times l \sim 0.06$  Å, which, being dynamically disordered, would appear only in the Debye-Waller factors, and are about half of the B-factor displacements at room temperature in  $NdNiO_3$ . The JT distortions required to explain the stiffening at the MIT are therefore compatible with the diffraction experiments: above the MIT they are disordered and account for half of the thermal/disordered displacements of the O atoms; below the MIT they are totally or partially absent due to the disproportionation of the JT  $Ni^{3+}$  into  $Ni^{3\pm\delta}$ , or simply frozen. This may also explain EXAFS experiments indicating that the splitting of the Ni–O bond lengths persist also above the MIT in  $RNiO_3$  with  $R = Pr, Nd, Eu$ .<sup>23</sup> This fact has been

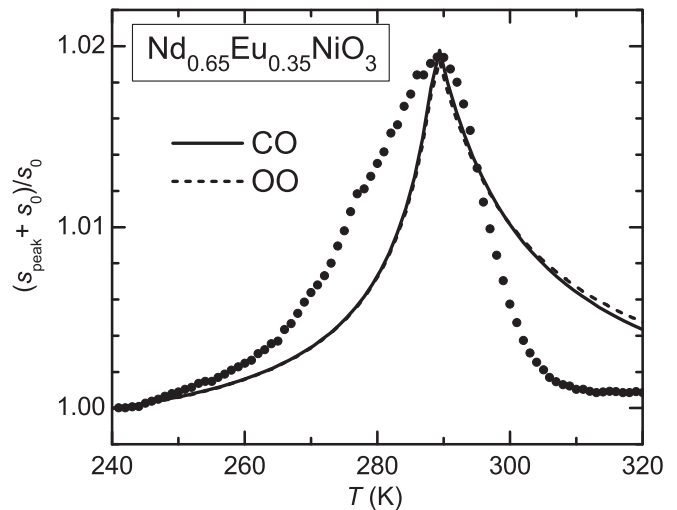


FIG. 4. Peaked component of  $s'$  (curve 3 of Fig. 3) fitted assuming CO or OO at 289 K.

explained in terms of localized CO phase also in the metallic state, but might be due to the disordered JT distortions. Another case where the anomalously large mean-square displacements suggest JT distortions is a recent neutron diffraction study on  $PrNiO_3$ .<sup>59</sup>

### I. The peaked softening at $T_{IM}$

Up to now we dealt with the steplike stiffening below the MIT, which however is accompanied by a peaked softening and absorption. The narrow shape of such an anomaly suggests that it is due to fluctuations associated with the MIT, but the absorption is almost independent of frequency, while the critical absorption is expected to be proportional to it.<sup>48</sup>

The real part of the peak, corresponding to curve 3 in Fig. 3, is plotted in Fig. 4 as  $s_{peak} + s_0$ , cleared of the step and temperature dependent part of the background. We tried to fit with the expressions appropriate for CO and OO, namely  $s = 1/(C_{CO/OO} + C_{bg})$  where  $C_{CO/OO}(T)$  is given by Eq. (5) above  $T_{CO}/T_{OO}$  and in Appendix B in the low temperature phase. The parameters were  $T_{CO} = T_{OO} = 289$  K,  $\Delta T = T_{JT} = 14.4$  K and  $C_0 \simeq 0.02$ ,  $C_{bg} = s_0^{-1} = 0.98$  for both cases. The resulting curves, very close to each other, fit very poorly the experimental data. In particular, the observed peak is steeper in the high temperature side, while the fitting curves are steeper in the low temperature phase, as expected. This discrepancy cannot be accounted for by relaxation of domain walls in the low temperature phase, since relaxations depend on the measuring frequency and the anomaly we observe does not. The failure of reproducing the peaked component as softening from OO or CO should be considered as an indication that the origin of the peak is different and we leave it as an open question.

## V. CONCLUSIONS

We measured the complex dynamic Young's modulus of  $NdNiO_3$  and  $Nd_{0.65}Eu_{0.35}NiO_3$ , in order to study the elastic anomalies associated with the MIT and magnetic transition. The main features are a sharp stiffening of  $\sim 6\%$  below the

MIT, perfectly reproducible during cooling and heating in  $\text{Nd}_{0.65}\text{Eu}_{0.35}\text{NiO}_3$  and with a broad hysteresis in  $\text{NdNiO}_3$ , accompanied by a narrow dip at the MIT. The change of the MIT between first- and second-order character at the two compositions agrees with the known phase diagram of  $R\text{NiO}_3$  as a function of the  $R$  size. The differences with respect to elasticity measurements on Mn perovskites are the absence of precursor softening associated with the MIT, the sharpness of the transition during heating or when it is second order, and the broadness of the hysteresis when it is first order. Both the narrow softening at the MIT and the stiffening below it seem not to be associated with spin ordering, which in the Eu-doped sample occurs at a temperature lower than the MIT.

By comparing cooling and heating runs, it was possible to separate the steplike stiffening from the other anomalies, which present similarities with the excess specific heat, and whose relationship with spin and charge order have been briefly considered. A fit of the dip at the MIT in terms of CO has been made, but its quality is too poor to draw a conclusion.

In order to explain the rather unusual steplike stiffening, possible mechanisms producing elastic anomalies at magnetic, charge order and orbital order transitions have been considered, and it is concluded that the stiffening is due to the disappearance or to freezing in the insulating phase of dynamic JT distortions, due to the charge disproportionation and ordering that accompanies the MIT and transforms JT active  $\text{Ni}^{3+}$  into  $\text{Ni}^{3\pm\delta}$ . The driving force for the MIT is not orbital ordering or any mechanism linearly coupled to strain, in view of the absence of precursor softening. This is in agreement with the idea that the MIT is caused by the opening of a gap when the orbital overlap drops below a threshold during cooling. In fact, such a mechanism depends only on the different thermal expansivities of the  $R$ -O and Ni-O bonds, and does not produce softening. The fluctuating tetragonal/orthorhombic Jahn-Teller distortion of the  $\text{NiO}_6$  octahedra necessary to justify the observed jump in the elastic modulus is estimated as  $\sim 3\%$  and the compatibility of such a requirement with other structural studies is discussed.

#### ACKNOWLEDGMENTS

The authors thank Marcia T. Escote and Fenelon M. Pontes for the preparation of the samples. F. C. wishes to thank P. M. Latino and F. Corvasce for their technical assistance in the experiments. This work was partially supported by the Brazilian agencies FAPESP and CNPq.

#### APPENDIX A

We determine the factor that connects the amplitude of softening in Eq. (6) to the anisotropy of the elastic quadrupole tensor of the octahedral distortions  $\Delta\lambda$ . This can be done by evaluating the relaxation of the reciprocal of the Young's modulus,  $\delta E^{-1}(\hat{\mathbf{n}})$ , along a generic direction  $\hat{\mathbf{n}}$  after application of a uniaxial stress  $\sigma = \sigma_0|\hat{\mathbf{n}}\rangle\langle\hat{\mathbf{n}}|$  and then performing the angular average of the relaxation strength,  $\delta E^{-1}(\hat{\mathbf{n}})/E^{-1}(\hat{\mathbf{n}})$ , over  $\hat{\mathbf{n}}$ , in order to obtain an approximation of the polycrystalline

average. It is convenient to decompose stress and strain into an orthonormal basis adapted to the cubic symmetry<sup>56</sup>

$$T^1 = \frac{1}{\sqrt{3}} \begin{bmatrix} 1 & 0 & 0 \\ 0 & 1 & 0 \\ 0 & 0 & 1 \end{bmatrix}, \quad (A1)$$

$$T^u = \frac{1}{\sqrt{6}} \begin{bmatrix} -1 & 0 & 0 \\ 0 & -1 & 0 \\ 0 & 0 & 2 \end{bmatrix}, \quad T^v = \frac{1}{\sqrt{2}} \begin{bmatrix} 1 & 0 & 0 \\ 0 & -1 & 0 \\ 0 & 0 & 0 \end{bmatrix}$$

where  $T^1$  is the dilatation (irreducible representation  $A_{1g}$ ),  $T^u$  and  $T^v$  tetragonal and orthorhombic shears of type  $E_g$ , and the three shears of type  $T_{2g}$  do not enter in the calculation, since they are orthogonal to the  $E_g$  JT distortion. The generic strain  $\varepsilon$  can be decomposed as  $|\varepsilon\rangle = \sum_\gamma \varepsilon_\gamma |T^\gamma\rangle$ , or explicitly  $\varepsilon_{ij} = \sum_\gamma \varepsilon_\gamma T_{ij}^\gamma$  with components  $\varepsilon_\gamma = \langle T^\gamma | \varepsilon \rangle$ , the scalar product being defined as  $\text{Tr}\{T^\gamma : \varepsilon\} = \sum_{ij} T_{ij}^\gamma \varepsilon_{ji}$ . Analogously, the uniaxial stress along  $\hat{\mathbf{n}}$  is decomposed as

$$\sigma_{ij} = \sigma_0 n_i n_j = \sum_\gamma \sigma_\gamma T_{ij}^\gamma.$$

Thanks to the orthonormality of the  $T^\gamma$  only the two components  $\sigma_u$  and  $\sigma_v$  will couple with  $\lambda^u$  and  $\lambda^v$  and we write them as

$$\sigma_u = \sigma_0 u, \quad \sigma_v = \sigma_0 v$$

with

$$u = \langle \hat{\mathbf{n}} | T^u | \hat{\mathbf{n}} \rangle = \frac{2n_{33}^2 - n_{11}^2 - n_{22}^2}{\sqrt{6}} \quad (A2)$$

$$v = \langle \hat{\mathbf{n}} | T^v | \hat{\mathbf{n}} \rangle = \frac{n_{11}^2 - n_{22}^2}{\sqrt{2}}.$$

The elastic quadrupoles of the two JT states are written as

$$\lambda^u = \lambda T^u, \quad \lambda^v = \lambda T^v$$

where  $\lambda$  gives the strength of the distortion.

The application of  $\sigma$  changes their elastic energies by  $d(E_u - E_v) = -v_0 \sum_{ij} (\lambda_{ij}^u - \lambda_{ij}^v) \sigma_{ji} = -v_0 \sigma_0 \lambda (u - v)$  and their populations,

$$n_u = e^{-E_u/k_B T} / (e^{-E_u/k_B T} + e^{-E_v/k_B T})$$

and  $n_v = 1 - n_u$  change as  $\frac{dn_u}{d\sigma_0} \simeq \frac{v_0}{4k_B T} \lambda (v - u)$ , where it is used  $\lambda \sigma \ll k_B T$ . This change of populations results in a change of the anelastic strain

$$d\varepsilon^{\text{an}} = c \sum_\gamma \lambda^\gamma dn_\gamma = \frac{\sigma_0 v_0 c}{4k_B T} \lambda^2 (u - v) [T^v - T^u].$$

The uniaxial component of  $d\varepsilon^{\text{an}}$  parallel to  $\hat{\mathbf{n}}$  is  $\langle \hat{\mathbf{n}} | d\varepsilon^{\text{an}} | \hat{\mathbf{n}} \rangle = \sum_{ij} n_i n_j d\varepsilon_{ij}^{\text{an}}$ , and using Eq. (A2) or  $\langle \hat{\mathbf{n}} | T^v - T^u | \hat{\mathbf{n}} \rangle = (u - v)$ , the relaxation of the Young's modulus along  $\hat{\mathbf{n}}$  is

$$\delta E^{-1}(\hat{\mathbf{n}}) = \frac{\langle \hat{\mathbf{n}} | d\varepsilon^{\text{an}} | \hat{\mathbf{n}} \rangle}{\sigma_0} = \frac{c v_0}{4k_B T} \lambda^2 (u - v)^2.$$

A simple formula for the polycrystalline average of the relaxation strength  $\Delta(\hat{\mathbf{n}}) = \delta E^{-1}(\hat{\mathbf{n}})/E^{-1}(\hat{\mathbf{n}})$  is obtained from the Reuss approximation of uniform stress over the grains,<sup>31</sup>



taking the angular average  $\langle \Delta \rangle \simeq \langle \delta E^{-1}(\hat{\mathbf{n}}) \rangle E$  where the anisotropy of the material is neglected. By using Eq. (A2) and  $\langle n_i^2 \rangle = \frac{1}{3}$ ,  $\langle n_i^4 \rangle = \frac{1}{5}$ ,  $\langle n_i^2 n_j^2 \rangle = \frac{1}{15}$  one finally obtains

$$\langle \Delta \rangle \simeq \frac{cv_0\lambda^2}{15k_B T} E.$$

It is possible to introduce a mixing of the two normalized symmetry strains, due to hybridisation with the  $O2p$  orbitals and delocalisation,<sup>60</sup> by setting  $\lambda^u = \lambda[(1 - \frac{f}{2})T^u + \frac{f}{2}T^v]$  and similarly for  $\lambda^v$  with  $0 \leq f \leq 1$ . In this case, in the above formulas  $\lambda$  should be replaced by  $\lambda(1 - f)$ , but from anelastic measurements it is not possible to evaluate  $\lambda$  and  $f$  independently, and we assume  $f = 0$ .

## APPENDIX B

The softening in Eq. (5) is valid above the CO or OO transition temperature; below that temperature, the restiffening depends on the precise nature of the transition. In the simplest cases of doublet OO,<sup>53</sup> the susceptibility below  $T_C$  is given by

$$\chi = \frac{1}{k_B T \cosh^2(h/k_B T)}$$

where  $h$  is the mean field felt by each ion, acting as order parameter, and is solution of the self-consistent equation

$$h = k_B T_C \tanh(h/k_B T).$$

For CO, consider the Landau expansion in terms of powers of the charge fluctuation order parameter, as in Ref. 47 but limiting to the case that only one order parameter  $Q$  is relevant. Then the free energy is written as

$$F = F_0 + \frac{\alpha}{2} Q^2 + \frac{\beta}{4} Q^4 + \frac{C_0}{2} \varepsilon^2 - g Q \varepsilon$$

where  $\alpha = \alpha_0(T - \Theta)$ . Solving the equilibrium conditions  $\partial F/\partial Q = 0$  and  $\partial F/\partial \varepsilon = 0$  one finds  $Q^2(T) = \alpha_0/\beta(T - T_{CO})$  with  $T_{CO} = \Theta + \Delta T$ ,  $\Delta T = g^2/(C_0\alpha_0)$ . The renormalized elastic constant is then

$$C = C_0 - g \frac{\partial Q}{\partial \varepsilon}$$

where  $\partial Q/\partial \varepsilon$  can be obtained by derivating with respect to  $\varepsilon$  the equation  $\partial F/\partial Q = 0$ :

$$\frac{\partial Q}{\partial \varepsilon} = \frac{g}{\alpha + 3\beta Q^2}.$$

When  $T > \Theta$  it is  $Q = 0$  and we obtain Eq. (5) as before, here rewritten as

$$C = C_0 \frac{(T - \Theta - \Delta T)}{(T - \Theta)}$$

In the CO phase, we obtain

$$C = C_0 \frac{(T - \Theta - \Delta T)}{(T - \Theta - \frac{3}{2}\Delta T)}.$$

These formulas have been used for the fits in Fig. 4.

<sup>1</sup>G. Catalan, *Phase Transitions* **81**, 729 (2008).

<sup>2</sup>Y. Bodenthin, U. Staub, C. Piamonteze, M. García-Fernández, M. J. Martínez-Lope, and J. A. Alonso, *J. Phys. Condens. Matter* **23**, 036002 (2011).

<sup>3</sup>S. B. Lee, R. Chen, and L. Balents, *Phys. Rev. Lett.* **106**, 016405 (2011).

<sup>4</sup>J. B. Torrance, P. Lacorre, A. I. Nazzari, E. J. Ansaldo, and Ch. Niedermayer, *Phys. Rev. B* **45**, 8209 (1992).

<sup>5</sup>M. Imada, A. Fujimori, and Y. Tokura, *Rev. Mod. Phys.* **70**, 1039 (1998).

<sup>6</sup>M. Tachibana, T. Yoshida, H. Kawaji, T. Atake, and E. Takayama-Muromachi, *Phys. Rev. B* **77**, 094402 (2008).

<sup>7</sup>M. L. Medarde, *J. Phys. Condens. Matter* **9**, 1679 (1997).

<sup>8</sup>J. A. Alonso, J. L. García-Muñoz, M. T. Fernández-Díaz, M. A. G. Aranda, M. J. Martínez-Lope, and M. T. Casais, *Phys. Rev. Lett.* **82**, 3871 (1999).

<sup>9</sup>J. L. García-Muñoz, M. A. G. Aranda, J. A. Alonso, and M. J. Martínez-Lope, *Phys. Rev. B* **79**, 134432 (2009).

<sup>10</sup>J. A. Alonso, M. J. Martínez-Lope, G. Demazeau, M. T. Fernández-Díaz, I. A. Presniakov, V. S. Rusakov, T. V. Gubaidulina, and A. V. Sobolev, *Dalton Trans.* **2008**, 6584.

<sup>11</sup>U. Staub, G. I. Meijer, F. Fauth, R. Allenspach, J. G. Bednorz, J. Karpinski, S. M. Kazakov, L. Paolasini, and F. d'Acapito, *Phys. Rev. Lett.* **88**, 126402 (2002).

<sup>12</sup>J. E. Lorenzo, J. L. Hodeau, L. Paolasini, S. Lefloch, J. A. Alonso, and G. Demazeau, *Phys. Rev. B* **71**, 045128 (2005).

<sup>13</sup>V. Scagnoli, U. Staub, M. Janousch, A. M. Mulders, M. Shi, G. I. Meijer, S. Rosenkranz, S. B. Wilkins, L. Paolasini, J. Karpinski, S. M. Kazakov, and S. W. Lovesey, *Phys. Rev. B* **72**, 155111 (2005).

<sup>14</sup>V. Scagnoli, U. Staub, A. M. Mulders, M. Janousch, G. I. Meijer, G. Hammerl, J. M. Tonnerre, and N. Stojic, *Phys. Rev. B* **73**, 100409 (2006).

<sup>15</sup>S. Di Matteo, *J. Phys.: Conf. Ser.* **190**, 012008 (2009).

<sup>16</sup>I. I. Mazin, D. I. Khomskii, R. Lengsdorf, J. A. Alonso, W. G. Marshall, R. M. Ibberson, A. Podlesnyak, M. J. Martínez-Lope, and M. M. Abd-Elmeguid, *Phys. Rev. Lett.* **98**, 176406 (2007).

<sup>17</sup>J.-G. Cheng, J.-S. Zhou, J. B. Goodenough, J. A. Alonso, and M. J. Martínez-Lope, *Phys. Rev. B* **82**, 085107 (2010).

<sup>18</sup>J.-S. Zhou, J. B. Goodenough, and B. Dabrowski, *Phys. Rev. B* **67**, 020404 (2003).

<sup>19</sup>S.-J. Kim, G. Demazeau, I. Presniakov, K. Pokholok, A. Baranov, A. Sobolev, D. Pankratov, and N. Ovanesyan, *Phys. Rev. B* **66**, 014427 (2002).

<sup>20</sup>I. Presniakov, G. Demazeau, A. Baranov, A. Sobolev, and K. Pokholok, *Phys. Rev. B* **71**, 054409 (2005).

<sup>21</sup>A. Caytuero, H. Micklitz, F. J. Litterst, E. M. Baggio-Saitovitch, M. M. Abd-Elmeguid, and J. A. Alonso, *Phys. Rev. B* **74**, 094433 (2006).

<sup>22</sup>A. Caytuero, H. Micklitz, M. M. Abd-Elmeguid, F. J. Litterst, J. A. Alonso, and E. M. Baggio-Saitovitch, *Phys. Rev. B* **76**, 193105 (2007).

- <sup>23</sup>C. Piamonteze, H. C. N. Tolentino, A. Y. Ramos, N. E. Massa, J. A. Alonso, M. J. Martínez-Lope, and M. T. Casais, *Phys. Rev. B* **71**, 012104 (2005).
- <sup>24</sup>P. Kalyani and N. Kalaiselv, *Sci. Technol. Adv. Mater.* **6**, 689 (2005).
- <sup>25</sup>J.-H. Chung, Th. Proffen, S. Shamoto, A. M. Ghorayeb, L. Croguennec, W. Tian, B. C. Sales, R. Jin, D. Mandrus, and T. Egami, *Phys. Rev. B* **71**, 064410 (2005).
- <sup>26</sup>A. Rougier, C. Delmas, and A. V. Chadwick, *Solid State Commun.* **94**, 123 (1995).
- <sup>27</sup>H. Hazama, T. Goto, Y. Nemoto, Y. Tomioka, A. Asamitsu, and Y. Tokura, *Phys. Rev. B* **62**, 15012 (2000).
- <sup>28</sup>H. Hazama, T. Goto, Y. Nemoto, Y. Tomioka, A. Asamitsu, and Y. Tokura, *Phys. Rev. B* **69**, 064406 (2004).
- <sup>29</sup>V. B. Barbeta, R. F. Jardim, M. S. Torikachvili, M. T. Escote, F. Cordero, F. M. Pontes, and F. Trequattrini, *J. Appl. Phys.* **109**, 07E115 (2011).
- <sup>30</sup>M. T. Escote, A. M. L. da Silva, J. R. Matos, and R. F. Jardim, *J. Solid State Chem.* **151**, 298 (2000).
- <sup>31</sup>A. S. Nowick and B. S. Berry, *Anelastic Relaxation in Crystalline Solids* (Academic Press, New York, 1972).
- <sup>32</sup>M. Asmani, C. Kermel, A. Leriche, and M. Ourak, *J. Eur. Ceram. Soc.* **21**, 1081 (2001).
- <sup>33</sup>R. A. Dorey, J. A. Yeomans, and P. A. Smith, *J. Eur. Ceram. Soc.* **22**, 403 (2002).
- <sup>34</sup>M. T. Escote, V. B. Barbeta, R. F. Jardim, and J. Campo, *J. Phys. Condens. Matter* **18**, 6117 (2006).
- <sup>35</sup>M. E. Lines, *Phys. Rep.* **55**, 133 (1979).
- <sup>36</sup>L. R. Testardi, *Phys. Rev. B* **12**, 3849 (1975).
- <sup>37</sup>R. Klingeler, J. Geck, R. Gross, L. Pinsard-Gaudart, A. Revcolevschi, S. Uhlenbruck, and B. Büchner, *Phys. Rev. B* **65**, 174404 (2002).
- <sup>38</sup>J. Blasco, M. Castro, and J. Garcia, *J. Phys. Condens. Matter* **6**, 5875 (1994).
- <sup>39</sup>J. Pérez, J. Blasco, J. García, M. Castro, J. Stankiewicz, M. C. Sánchez, and R. D. Sánchez, *J. Magn. Magn. Mater.* **196–197**, 541 (1999).
- <sup>40</sup>C. X. Chen, R. K. Zheng, T. Qian, Y. Liu, and X. G. Li, *J. Phys. D: Appl. Phys.* **38**, 807 (2005).
- <sup>41</sup>S. Seiro, H. R. Salva, M. Saint-Paul, A. A. Ghilarducci, P. Lejay, P. Monceau, M. Nunez-Regueiro, and A. Sulpice, *J. Phys. Condens. Matter* **14**, 3973 (2002).
- <sup>42</sup>S. Zvyagin, H. Schwenk, B. Lüthi, K. V. Kamenev, G. Balakrishnan, D. McK. Paul, V. I. Kamenev, and Yu. G. Pashkevich, *Phys. Rev. B* **62**, 6104 (2000).
- <sup>43</sup>J.-S. Zhou, J. B. Goodenough, B. Dabrowski, P. W. Klamut, and Z. Bukowski, *Phys. Rev. Lett.* **84**, 526 (2000).
- <sup>44</sup>W. Rehwald, *Adv. Phys.* **22**, 721 (1973).
- <sup>45</sup>A. Bulou, M. Rousseau, and J. Nouet, *Key Eng. Mater.* **68**, 133 (1992).
- <sup>46</sup>M. A. Carpenter and E. H. K. Salje, *Eur. J. Mineral.* **10**, 693 (1998).
- <sup>47</sup>T. Goto and B. Lüthi, *Adv. Phys.* **52**, 67 (2003).
- <sup>48</sup>B. Lüthi, *Physical Acoustics in the Solid State*, Springer Series in Solid-State Sciences (Springer, Berlin, 2007).
- <sup>49</sup>M. Long Jr., A. R. Wazzan, and R. Stern, *Phys. Rev.* **178**, 775 (1969).
- <sup>50</sup>U. Kawald, O. Mitze, H. Bach, J. Pelz, and G. A. Saunders, *J. Phys. Condens. Matter* **6**, 9697 (1994).
- <sup>51</sup>S. Morita, H. Higaki, I. Ishii, M. Takemura, F. Iga, T. Takabatake, M. Tsubota, and T. Suzuki, *Physica B* **383**, 43 (2006).
- <sup>52</sup>M. Poirier, F. Laliberté, L. Pinsard-Gaudart, and A. Revcolevschi, *Phys. Rev. B* **76**, 174426 (2007).
- <sup>53</sup>R. L. Melcher, *Physical Acoustics*, edited by W. P. Mason and R. N. Thurston (Academic Press, New York, 1976), p. 1.
- <sup>54</sup>F. Cordero, *Phys. Rev. B* **47**, 7674 (1993).
- <sup>55</sup>H. Köppel, D. R. Yarkony, and H. Barentzen, *The Jahn-Teller Effect - Fundamentals and Implications for Physics and Chemistry* (Springer, Heidelberg, 2009).
- <sup>56</sup>G. Leibfried and N. Breuer, *Point Defects in Metals I* (Springer, Berlin, 1978).
- <sup>57</sup>O. G. Brandt and C. T. Walker, *Phys. Rev.* **170**, 528 (1968).
- <sup>58</sup>K. I. Kugel and D. I. Khomskii, *Sov. Phys. Usp.* **25**, 231 (1982).
- <sup>59</sup>M. Medarde, M. T. Fernández-Díaz, and Ph. Lacorre, *Phys. Rev. B* **78**, 212101 (2008).
- <sup>60</sup>N. Binggeli and M. Altarelli, *Phys. Rev. B* **70**, 085117 (2004).